Flexible all-solid-state supercapacitors based on PPy/rGO nanocomposite on cotton fabric

Shuzhen Xu[a], Huilian Hao[a,*], Yinan Chen[a], Wenyao Li[a,b,*], Wenzhong Shen[d], Paul R. Shearing[b] and Dan J. L. Brett[b], Guanjie He[b,c] *

[a] *College of Material Engineering, Shanghai University of Engineering Science 333 Long Teng Road, Shanghai 201620, China*

[b] *Electrochemical Innovation Lab, Department of Chemical Engineering, University College London, London WC1E 7JE, United Kingdom.*

[c] *School of Chemistry, University of Lincoln, Joseph Banks Laboratories, Green Lane, Lincoln, LN6 7DL, United Kingdom.*

[d] *Institute of Solar Energy, and Key Laboratory of Artificial Structures and Quantum Control (Ministry of Education), Department of Physics and Astronomy, Shanghai Jiao Tong University, 800 Dong Chuan Road, Shanghai 200240, China*

*Corresponding author, E-mail: sulee8866@126.com (Huilian Hao); wenyao.li@ucl.ac.uk (Wenyao Li); g.he@ucl.ac.uk (Guanjie He)

Abstract: Polypyrrole (PPy) has high electrochemical activity and low cost, so it has great application prospects in wearable supercapacitors. Herein, we have successfully prepared polypyrrole/reduced graphene oxide (PPy/rGO) nanocomposite cotton fabric (NCF) by chemical polymerization, which exhibits splendid electrochemical performance compared with the individual. The addition of rGO can block the deformation of PPy caused by the expansion and contraction. The as-prepared PPy-0.5/rGO NCF electrode exhibits the brilliant specific capacitance (9300 mF cm^{-2} at 1 mA cm^{-2}) and the capacitance retention with 94.47% after 10000 cycles. At the same time, the superior capacitance stability under different bending conditions and reuse capability have been achieved. All-solid-state supercapacitor has high energy density of 167 μWh cm^{-2} with a power density of 1.20 mW cm^{-2}. Therefore, the PPy-0.5/rGO NCF electrode has a broad application prospect in high-performance flexible supercapacitor fabric electrode.

Keywords: PPy; PPy/rGO nanocomposite; Cotton fabric electrode; Symmetric all-solid-state supercapacitor

1. Introduction

With the progress of society, the requirements for lightweight, high energy density and safe energy storage equipment are increasing day by day [1-4]. The supercapacitor is a new type of energy storage unit integrating the advantages of battery and traditional capacitor, which has high energy density, long cyling life and low maintenance cost [5-8]. Traditional supercapacitors hardly satisfy the application needs of flexible and wearable devices due to their rigidity [9, 10]. Lately, high-performance supercapacitors with flexibility, durability, lightweight and stretchability been rapidly developed, which have become energy storage units of wearable devices [11-13]. The key to manufacturing flexible supercapacitors is to fabricate electrodes with good electrochemical property and mechanical stability. Hence, the preparation of high-performance fabric electrodes is a critical breakthrough [14, 15].

Yarn [16], fiber [17], metal wire [18], paper [19], film [20] and cotton fabric [21] can be treated as flexible electrode substrates. Among these materials, cotton fabric based electrodes have attracted more and more attention due to their characteristics of lightweight, comfort, low-cost, good water absorption and excellent mechanical strength [22, 23]. Nevertheless, the electrical insulating property limits the application of cotton fabrics in supercapacitors, so it is urgent to find a solution to make conductive cotton fabric materials for meeting the requirement of the flexible electrode [24, 25]. Various coating processes are the most commonly used methods for converting cotton fabric into conductive fabric materials. Coating traditional electrode materials like carbon materials [26], metal materials [27], conductive polymers [28] on the fabric to form flexible supercapacitor electrodes is an effective method.

For the past few years, many researchers have turned their attention to the integration of carbon materials and conductive polymers, the composite material benefits from their respective advantages [29]. On the one hand, carbon materials have large electrical double layer capacitance, high surface area and stable structure, which prevents the expanding and shrinking of the conducting polymers [30], thereby improving the cycle performance [31]. Additionally, the introduction of conducting

polymers in composite materials can improve the capacitance, conductivity and energy density [32].

To improve the electrochemical porperties, many methods of preparing reduced graphene oxide/polypyrrole (rGO/PPy) composites have been studied. As an example, M. Barakzehi *et al.* prepared PET/rGO-5/PPy by the dipping and drying approach, the capacitance remained 76% after 6000 cycles. The specific capacitance of the supercapacitor is 230 mF cm^{-2} at 1 mV s^{-1}, with energy density 11 μWh cm^{-2} and power density 0.03 mW cm^{-2} [33]. Chen *et al*. fabricated rGO/PPy composite films by using the electrodeposition method. Its specific capacitance is 411 mF cm^{-2} at 0.2 mA cm^{-2} and the capacitance retention is 80% after 5000 cycles. The solid-state supercapacitor exhibits an energy density of 20 μWh cm^{-2} with the power density of 0.04 mW cm^{-2} [34]. The, fabric substrate has the advantage of lightweight, comfort and good mechanical strength, which is used to construct flexible electrodes. Lv *et al*. successfully prepared the PPy-coated cotton electrodes, which has the areal specific capacitance with 5073 mF cm^{-2} at 1 mA cm^{-2} and remained 90% of its original capacitance after 5000 cycles [11]. Sun *et al*. fabricated PPy/CCF flexible electrodes through the in-situ electrodeposition method has the specific capacitance with 3596 mF cm^{-2} at 2 mA cm^{-2} and the capacitance retention with 96.50% after 4000 cycles [1]. However, there are currently little literatures on the use of the lightweight and low-cost characteristics of cotton fabric to construct PPy/rGO composite cotton fabric electrode. Moreover, a simple, low-cost preparation method of cotton fabric electrodes is needed to meet the applications of flexible supercapacitors.

Herein, we have successfully fabricated the PPy cotton fabric electrodes with different pyrrole monomer/ferric chloride reacting mole ratios (PPy-0.3 PPy-0.5 PPy-1.0 PPy-1.5 PPy-2.0) by a simple and low-cost chemical polymerization. The optimized electrode (PPy-0.5) was used to combine with rGO. The as-prepared PPy-0.5/rGO nanocomposite cotton fabric (NCF) can provide a short ion transport path and offer outstanding electrochemical performance, which displays splendid specific capacitance with 9300 mF cm^{-2} at 1 mA cm^{-2}, outstanding cycling stability with capacitance retention of 94.47% after 10000 cycles, the excellent flexibility and reusability.

Furthermore, symmetric supercapacitor prepared with two PPy-0.5/rGO NCF electrodes can achieve the maximal energy density of 167 μWh cm^{-2} with the power density of 1.20 mW cm^{-2}, the maximal power density can reach 6 mW cm^{-2} with energy density maintaining 11.66 μWh cm^{-2} and the capacitance retention with 81.39% after 10000 cycles. This study offers a lightweight and low-cost flexible cotton fabric electrode, which is expected to be a candidate electrode for flexible devices.

2. Experimental section

2.1 Materials

Graphite was procured from Sinopharm. Pyrrole, ferric trichloride, sodium 5-sulfosalicylate (NaSSA) and absolute ethanol was procured from the Aladdin reagent. Cotton fabric was received from Ao Bang Ltd. All the other reagents were used according to the original standard without any further purification.

2.2 Preparation of PPy and PPy/rGO NCF electrodes

PPy fabric electrodes were fabricated with cotton fabrics (5 cm × 5 cm) as substrate through the chemical polymerization method. In brief, the solution of ferric chloride, NaSSA (10 mL) and a piece of cotton fabric were frozen to ~ -5 ºC. Pour the pyrrole monomer (0.36 M) into the above mixture and let it stand for polymerization. Finally, the fabric was washed and dried at 60 ºC for 12 h, and thus PPy fabric electrode can be obtained. For better performance, five PPy fabric electrodes were prepared with the molar ratio of pyrrole monomer to ferric chloride as 0.3, 0.5, 1.0, 1.5 and 2.0 and named by PPy-0.3, PPy-0.5, PPy-1.0, PPy-1.5 and PPy-2.0, respectively.

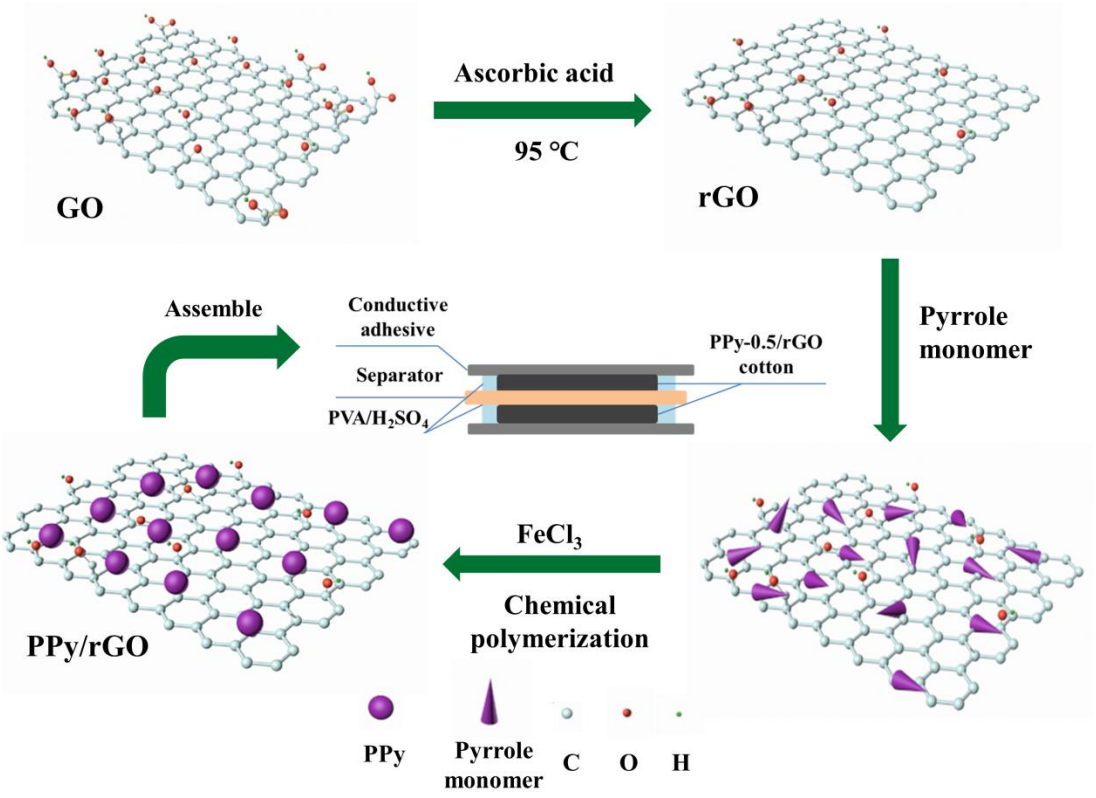

Fig. 1 Schematic of preparing the PPy-0.5/rGO NCF and all-solid-state supercapacitor assembled by two PPy-0.5/rGO NCF electrodes.

The above chemical polymerization method was applied to synthesize PPy/rGO NCF. The fabrication schematic diagram is shown in Fig. 1. Graphene oxide (GO) was obtained by the modified Hummers procedure [35]. Similarly, the pristine cotton substrate was put into the GO solution (5 mg ml^{-1}) at 70 ºC for 1 h, then dried at 80 ºC for 1 h. The GO-cotton fabric was prepared by repeating the above procedure several times. The reduction of GO to rGO was performed by using ascorbic acid (100 mM) as a safe reducing agent, the chemical reaction continued 15 minutes at 95 ºC. The resulting rGO-cotton was washed and dried at 80 ºC for 30 minutes. The rGO-cotton was immersed in the mixture of ferric chloride and NaSSA to freeze (-5 ºC). Pyrrole monomer was poured into the above frozen mixture and maintained statically at about 0-5 ºC for polymerization. Finally, the obtained PPy/rGO NCF electrode was washed then dried at 60 ºC for 12 h.

2.3 Characterization

The microstructures of fabric electrodes were researched by scanning electron microscope (SEM, S-4800) and high-resolution transmission electron microscope (HRTEM, JEM-2100, JEOL). The molecular structure of electrodes was characterized by Raman spectroscopy (Lab RAM, HR800) and Fourier transform infrared spectroscopy (FTIR, NEXUS-820). The chemical states of electrodes were studied by X-ray photoelectron spectroscopy with Thermo scientific K-alpha surface analysis.

2.4 Assembly of all-solid-state supercapacitors

5 g polyvinyl alcohol (PVA) and 5 g H_2SO_4 were put into 50 mL DI water and heated to 90 ºC at vigorous stirring until the solution became clear to form PVA/H2SO4 gel electrolyte. The supercapacitor was assembled as follows: two PPy/rGO cotton fabric electrodes (1 cm × 1 cm) were submerged in gel electrolyte for 1 h, then parallelly located on cellulosic paper sandwiched between two PPy/rGO NCF and the conductive adhesives were used as current collectors for supercapacitor. Finally, the supercapacitor was left to dry at room temperature, as shown in Fig. 1.

2.5 Electrochemical measurements

To study the electrochemical properties of the cotton fabric electrode, cyclic voltammetry (CV), galvanostatic charge-discharge (GCD) and electrochemical impedance spectroscopy (EIS) were measured on a CHI660E electrochemical workstation. The as-prepared cotton fabric electrode (1 cm × 1 cm) serves as working electrode, Pt sheet and saturated Ag/AgCl electrode serve as counter electrode and reference electrode. The electrochemical properties measurements of all-solid-state supercapacitor was carried out in a two-electrode

Based on the CV curves, the areal specific capacitance (mF cm^{-2}) can be calculated as:

$$C_{areal} = \frac{\int I(V)dV}{A \cdot v \cdot \Delta V} \quad (1)$$

Where v is the scan rate (mV s^{-1}), ΔV is the voltage range (V) and A is the active area (cm^2).

The areal specific capacitance (mF cm^{-2}) can be calculated according to the GCD test by the following formula:

$$C_S = \frac{I \times \Delta t}{S \times \Delta V} \quad (2)$$

Where I (mA) is discharge current, Δt (s) is discharge time, S (cm^2) is an active area and ΔV (V) is the potential window.

The energy density and power density can be attained based on formulas (3) and (4), respectively.

$$E = \frac{C_S \times (\Delta V)^2}{2 \times 3.6} \quad (3)$$

$$P = \frac{3600 \times E}{\Delta t} \quad (4)$$

Where E (Wh·cm^{-2}) is the energy density, P (W·cm^{-2}) is the power density, C_S (F cm^{-2}) is the areal specific capacitance of supercapacitor, ΔV (V) is the potential window of supercapacitor and Δt (s) is the discharge time.

3. Results and discussion

3.1 Characterization and analysis

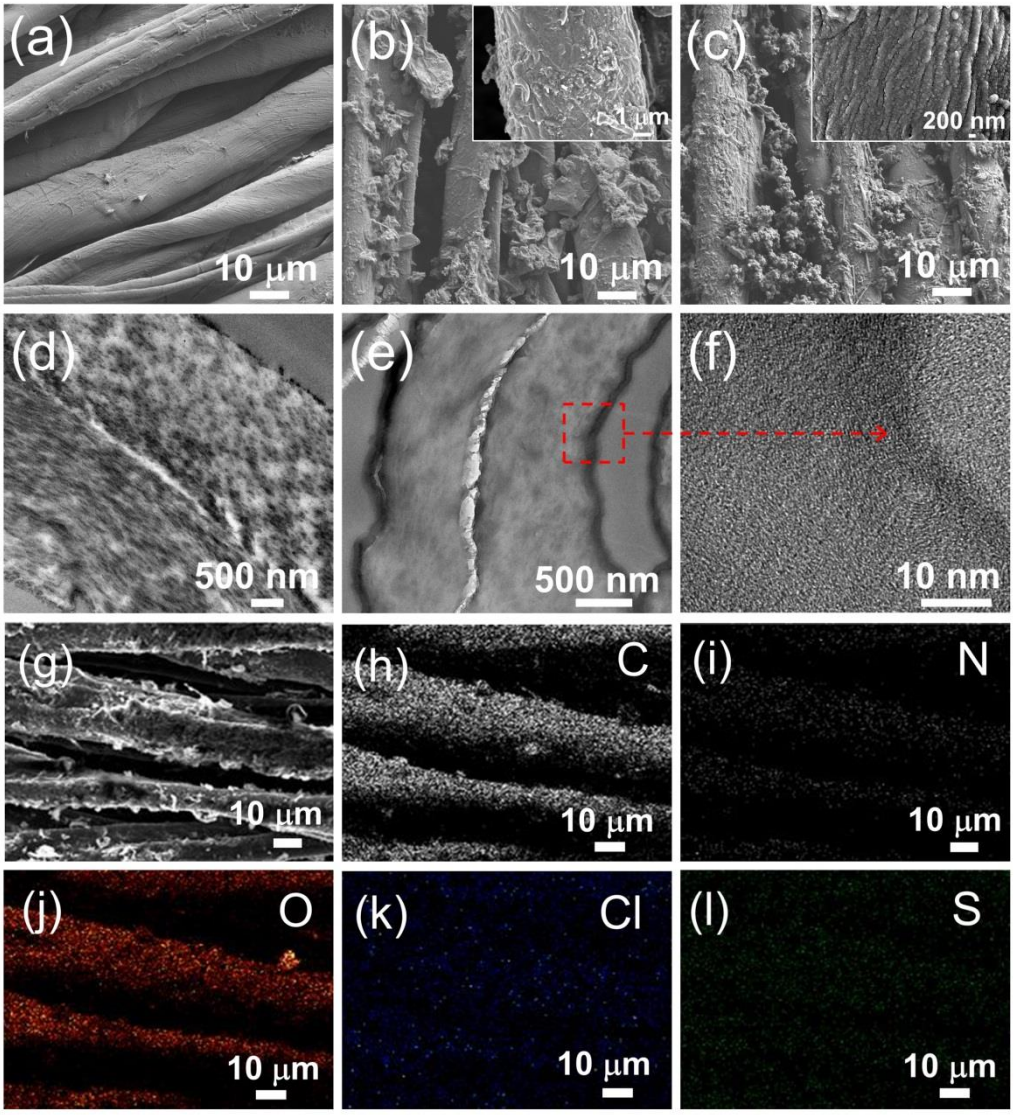

Fig. 2 SEM images of (a) pristine cotton fabric, (b) PPy cotton fabric and (c) PPy/rGO NCF (Insets show the higher magnification images). TEM images of (d) PPy cotton fabric, (e) PPy/rGO NCF and (f) the corresponding to enlarged view of PPy/rGO NCF. The element mapping images of PPy/rGO NCF electrode (g-l).

Fig. 2 exhibits the morphologies of pristine cotton fabric, PPy and PPy/rGO NCF. From Fig. 2a, we can see that the surface of the pristine cotton fabric is smooth and neat and the texture of the pristine cotton fabric surface can be seen. In Fig. 2b, because the PPy successfully grew on the surface of the pristine cotton fabric by chemical polymerization, the surface of the fabric becomes rough and exhibits a massive PPy

coating. After rGO loading and PPy polymerization, a dense and thick layer is formed, which is composed of numerous nanoparticles with sizes of ~ 10-100 nm (Fig. 2c). In addition, the rGO is tightly integrated with PPy through the non-covalent π-π stacking, as displayed in the inset of Fig. 2c. The rGO with the high surface area makes numerous conductive routes that can associate with the PPy nanoparticles to set up effective linkages and promote π-π stacking on the interface, providing an effective connection and dependable path for charge transfer [33]. Compared with the PPy cotton fabric electrode, PPy/rGO NCF has smaller nanoparticles (as shown in Fig. 2b and 2c), which provides the possibility to boost the specific capacitance of composites. Thus, PPy/rGO NCF electrode has great potential to enhance the overall performance.

Morphologies of the PPy and PPy/rGO NCF were further studied by TEM. From Fig. 2d, the PPy is uniformly grown onto the fabric, which matches very well with relevant SEM images in Fig. 2b. The wrinkles and corrugations of rGO are apparent in Fig. S1, demonstrating a typical rGO based three-dimensional structure [5]. The stable connection between PPy and rGO is critical to the capacitance performance of fabric electrodes. As exhibited in Fig. 2e, the edge of the PPy/rGO NCF is evident thicker than the PPy fabric in Fig. 2d, suggesting the distribution of the PPy nanoparticles on the surface rGO forms a close connection. The good contact between the PPy nanoparticles and rGO can establish channels in PPy/rGO NCF electrodes, which can efficiently offer a short ion diffusion routes and plentiful active sites. Besides, the dark areas corresponding to the thick edge of the PPy/rGO nanocomposite can be observed in Fig. 2f, which further confirms the successful combination of PPy and rGO. Additionally, homogeneous distribution of carbon, nitrogen, oxygen, chlorine and sulfur of PPy/rGO NCF electrode can be observed in Fig. 2(g-l), the grey, white, red, blue and green dots correspond to the carbon, nitrogen, oxygen, chlorine, and sulfur element, respectively.

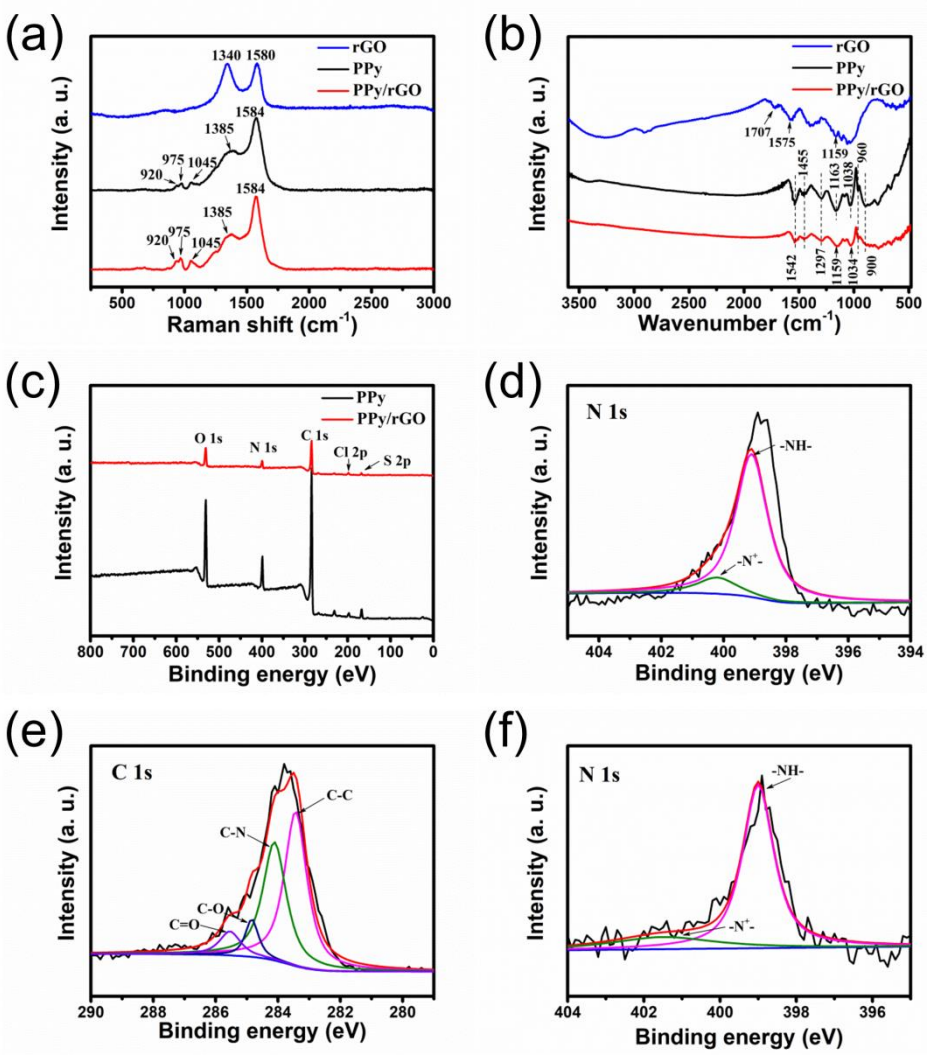

Fig. 3 (a) Raman spectra of rGO, PPy and PPy/rGO NCF. (b) FTIR spectra of rGO, PPy and PPy/rGO NCF. (c) XPS scan spectra of PPy and PPy/rGO NCF. (d) High-resolution N 1s spectrum of PPy fabric. (e, f) High-resolution C 1s and N 1s spectra of PPy/rGO NCF.

The molecular configuration of rGO, PPy and PPy/rGO NCF can be measured by Raman spectroscopy. Fig. 3a displays the Raman spectra of PPy, rGO and PPy/rGO NCF. The Raman spectrum of rGO cotton fabric shows G and D peaks at 1580 and 1340 cm^{-1}. The G peak relates to the vibration of sp^2 carbon atoms and the D peak corresponds to the disorder and defects owing to the vibrations of sp^3 carbon atoms [36]. The spectra of PPy and PPy/rGO NCF show similar shapes and both demonstrate prominent peaks corresponded to PPy, the peak around at 920, 975 1045 1385 and 1584

cm^{-1} can be assigned to the quinoid polaronic, bipolaronic structure, the C-H in-plane deformation, ring stretching pattern of the polymer backbone and the C=C backbone stretching, respectively. It should be noted that the D band (1340 cm^{-1}) and G band (1580 cm^{-1}) of rGO were overlapped by the peaks of PPy in the PPy/rGO NCF [37]. Compared with PPy cotton fabric, the peak at 1385 cm^{-1} of PPy/rGO NCF is reinforced, indicating that there is a tight interaction between rGO and PPy good consistent with the SEM result in the inset of Fig. 2c [38]. In addition, the absorption band intensity ratio (I_{1385}/I_{1584}) reflects the relative conjugate length of the PPy molecular chain [11]. The I_{1385}/I_{1584} ratio is 1.03 and 2.88 for PPy and PPy/rGO fabric, respectively. The higher intensity ratio value indicates that the conjugate length of the PPy chains is lengthened, the more stable the resulting molecule. The Raman spectra of all the PPy fabric are exhibited in Fig. S2, and the I_{1385}/I_{1584} of PPy-0.3, PPy-0.5, PPy-1.0, PPy-1.5 and PPy-2.0 cotton fabric electrodes is 0.85, 1.03, 0.78, 0.70, and 0.68, respectively. Videlicet, PPy-0.5 cotton fabric electrode is the most stable among the PPy fabric.

Fig. 3b exhibits the infrared spectra of PPy, rGO and the PPy/rGO nanocomposite. For rGO cotton fabric, the peaks at 1575 and 1159 cm^{-1} ascribe to the C=C stretching and C-O stretching vibrations, respectively [37, 39]. The peak of GO relating to -OH (at ~3438 cm^{-1}) can not be noted and the peak at 1707 cm^{-1} relating to the C=O stretching vibration of carbonyl becomes weak. Compared to other characteristic peaks in the spectrum of PPy cotton fabric, oxygen-containing functional groups weakened or disappeared, suggesting that GO has been successfully reduced [39]. This conversion results in restoration of the π-conjugation and electron delocalization in the carbon layers, which can promote conductivity [33]. The FTIR absorption spectrum of PPy cotton fabric electrode shows the peak at ~ 1542 cm^{-1} attributing to C=C stretching vibrations of pyrrole ring, 1455 cm^{-1}, 1297 cm^{-1} and 1163 cm^{-1} ascribing to the C-N stretching vibration of PPy, 1038 cm^{-1} relating to C-H in-plane bending of PPy ring, 960 cm^{-1} attributing to C-C out of plane ring deformation as well as 900 cm^{-1} attributing to ring deformation [33, 37, 38, 40]. All these characteristic peaks reveal that PPy was successfully prepared. For spectrum of the PPy/rGO NCF electrode, as expected, the characteristic peaks at ~ 1542, 1455, 1297, 960 and 900 cm^{-1} of PPy appear in the

PPy/rGO nanocomposite absorption spectrum, which suggests that PPy exists in PPy/rGO nanocomposites. It also can be observed that the characteristic bands at 1159 cm^{-1} are attributing to C-O stretching vibrations of rGO. Compared with the absorption band of PPy, the peak at 1038 cm^{-1} corresponding to C-H in-plane bending of PPy ring downshifts to 1034 cm^{-1}, demonstrating the successful combination of PPy and rGO [41].

The modification of compositions and chemical states of the fabric electrodes can be explored by XPS measurements. Fig. 3c displays the XPS scan spectra of PPy and PPy/rGO nanocomposite. The carbon, nitrogen, oxygen, chlorine, and sulfur can be observed, corresponding well to the element mapping images in Fig. 2d-f. PPy and PPy/rGO exhibit prominent peaks at ~ 284, 399 and 532 eV attributing to C 1s, N 1s, and O 1s [42, 43], demonstrating that PPy was successful by the chemical polymerization. This results are in accordance with the above Raman and FTIR. Fig. 3d illustrates the N 1s binding energy spectra of PPy. The fitted peaks at ~ 399.1 eV and 400.2 eV relate to the N-H nitrogen atom in the main chain of PPy and the $-N^+-$ cation. The $-N^+-$ is critical to the conductive property of PPy due to the electrostatic interaction between the positive charge and electron promotes conductivity. Fig. 3e shows the experimental C 1s spectrum black solid line of PPy/rGO NCF electrode, the fitted peaks red solid lines at 283.4, 284.1, 284.8 and 285.5 eV relate to C-C, C-N, C-O and C=O, respectively. The C-N (~ 284.1 eV) at C 1s XPS spectrum of PPy/rGO nanocomposite originates from PPy, demonstrating the existence of PPy. The results are consistent with FTIR. The N 1s spectrum for PPy/rGO NCF electrode in Fig. 3f can be fitted two peaks with 399.8 and 401.5 eV, corresponding to the chemical bonds amine (-NH-) and positively charged nitrogen ($-N^+-$). Compared with the N 1s XPS spectrum of PPy cotton fabric electrode, the fitted peaks shifted to a higher region. It could be caused by the π-π stacking between the rGO and PPy. Moreover, N element content decreases from about 10.68 at.% in the PPy to 9.54 at.% in the PPy/rGO, indicating the existence of rGO in the PPy/rGO NCF electrode [41]. The above XPS results demonstrate that PPy/rGO nanocomposite has been successfully prepared.

3.2 Electrochemical analyses

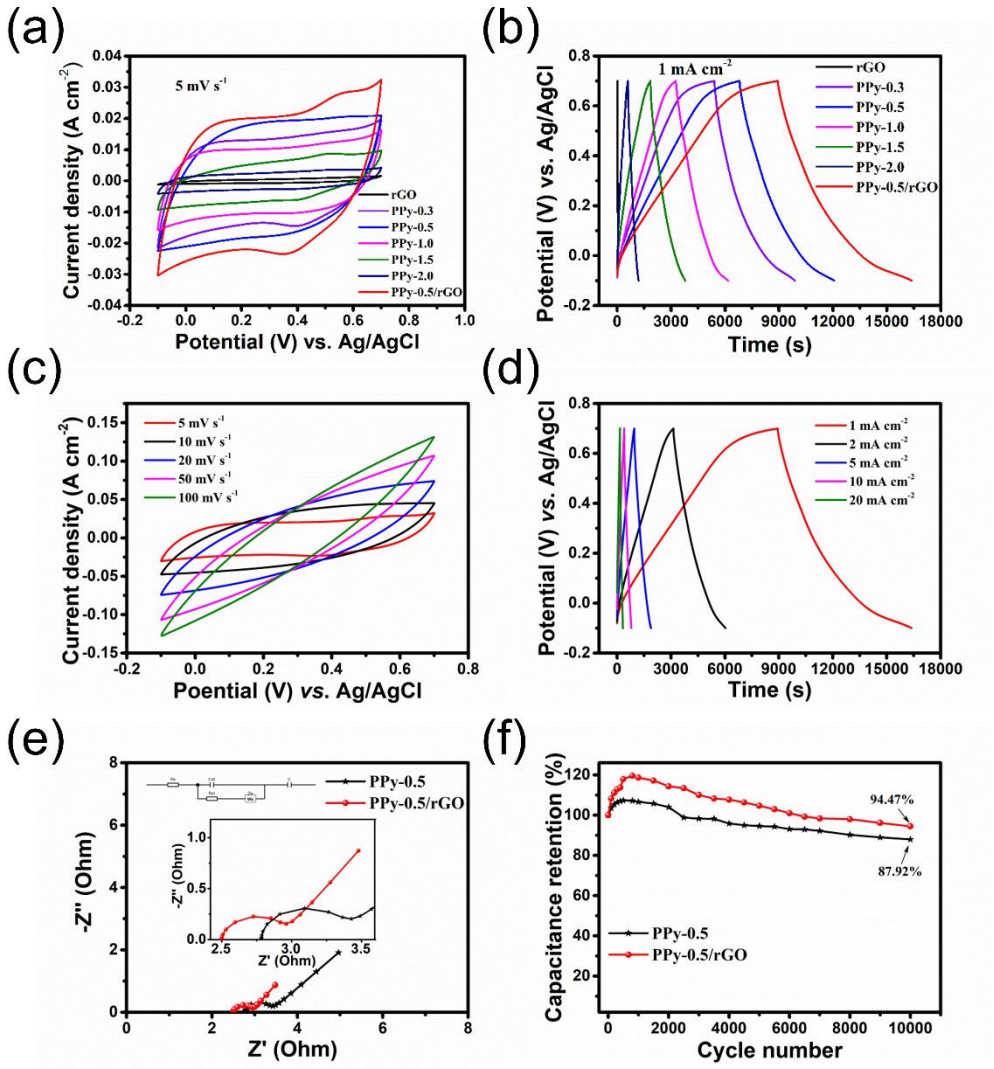

Fig. 4 (a) CV and (b) GCD curves of rGO, PPy-0.3, PPy-0.5, PPy-1.0, PPy-1.5, PPy-2.0 and PPy-0.5/rGO cotton fabric electrodes at 5 mV s^{-1} and 1 mA cm^{-2}. (c) CV and (d) GCD curves of PPy-0.5/rGO cotton fabric electrode at various scan rates and current densities. (e) Nyquist plots for PPy-0.5 and PPy-0.5/rGO cotton fabric, insets are the enlarged diagram and equivalent circuit model, respectively. (f) Capacitance retention of PPy-0.5 and PPy-0.5/rGO cotton fabric electrodes after 10000 cycles at 50 mV s^{-1}. All the electrodes were studied in the three-electrode system using 1.0 M H_2SO_4 as the electrolyte.

Fig. 4a exhibits the CV curves of PPy cotton fabric electrodes with different ratios

at 5 mV s^{-1}. The closed curve area of the PPy-0.5 cotton fabric electrode is significantly bigger than those of other PPy cotton fabric electrodes with different ratios, indicating the PPy-0.5 cotton fabric electrode has the higher areal specific capacitance. Meanwhile, the CV curves of all PPy cotton fabric electrodes at different scan rates are exhibited in Fig. S3. It shows that the PPy-0.5 cotton fabric electrode has the biggest current densities among all the PPy cotton fabric electrodes with different ratios, which further demonstrates the highest areal specific capacitance of the PPy-0.5 fabric electrode [36]. This is due to the fact that when increasing the ratio of PPy cotton fabric electrode, the PPy nanoparticles gradually aggregate, which prevents diffusion of ions and increases resistance as the ratio increases [44].

Fig. 4b displays the GCD curves of all PPy cotton fabric electrodes at the current density of 1.0 mA cm^{-2}. The PPy-0.5 cotton fabric electrode has longer discharge time than other PPy cotton fabric electrodes with different ratios, suggesting greater specific capacitance. Besides, the GCD curves of all the as-prepared PPy cotton fabric electrodes at various current densities are exhibited in Fig. S3. The discharge time of PPy-0.5 cotton fabric electrodes is longer than that of other PPy cotton fabric electrodes with different ratios at each current density, which further indicates that PPy-0.5 cotton fabric electrode has larger specific capacitance, the results agree with the CV in Fig. 4a. The areal specific capacitances of fabric electrodes are calculated from GCD measurements in Fig. 4b by using equation (2), and the corresponding values are ~ 175, 5587, 6583, 3636, 2415 and 746 mF cm^{-2} for the rGO, PPy-0.3, PPy-0.5, PPy-1.0, PPy-1.5 and PPy-2.0 cotton fabric electrodes at 1 mA cm^{-2}, respectively.

Based on the above results, PPy-0.5 was selected to combine with rGO to prepare the PPy-0.5/rGO nanocomposite electrode material. As shown in Fig. 4a, the PPy-0.5/rGO NCF electrode has the largest enclosed CV curve among all the as-prepared PPy and rGO cotton fabric electrodes, suggesting the highest areal specific capacitance. The significant capacitance enhancement of PPy-0.5/rGO NCF electrode suggests the rGO plays an important role in enhancing areal specific capacitance of PPy-0.5/rGO nanocomposite, which can be explained as follows: on the one hand, the existence of rGO provides higher electrical double layer capacitance contribution; additionally, rGO

can increase charge storage and decrease the internal resistance of the composite materials [33].

For further study of the electrochemical property of PPy-0.5/rGO NCF electrodes, the specific capacitances can be computed from the GCD curve (in Fig. 4b). The calculated capacitance of the PPy-0.5/rGO NCF electrode is identified as 4025 mF cm^{-2} at 20 mA cm^{-2}, which has the large specific capacitance and shows good rate performance. To evaluate the rate capability of all electrodes, the areal specific capacitances of all fabric electrodes at various current densities are gained and shown in Fig. S4. Among all the cotton fabric electrodes, the significant improvement of the specific capacitance of PPy-0.5/rGO NCF electrode manifests that the synergistic effect between rGO and PPy remarkably improves the energy storage of nanocomposite fabric electrode. This is due to that the combination of rGO and PPy can increase the charge storage, reduce the internal resistance and form fast electronic and ionic transmission channels [44].

To quest the practicability of the PPy-0.5/rGO nanocomposite for cotton fabric electrode, the CV was investigated within 5-100 mV s^{-1} and GCD was measured with current densities of 1-20 mA cm^{-2}. As exhibited in Fig. 4c, at all scan rates from 5-100 mV s^{-1}, the symmetrical quasi-rectangular CV curves can be observed and the shapes of the curves keep almost unchanged within the whole scan rates, indicating good capacitance behavior and outstanding rate performance. Fig. 4d presents the GCD of the PPy-0.5/rGO NCF electrode at various current densities. All the curves have nearly triangular shapes and small IR drops, revealing outstanding reversibility and low internal resistance. The calculated areal specific capacitances of PPy-0.5/rGO NCF electrode from equation (2) are 9300, 7237, 5787, 4912 and 4025 mF cm^{-2} at 1, 2, 5, 10 and 20 mA cm^{-2}, respectively.

For further investigation of all the PPy and PPy-0.5/rGO NCF electrodes, EIS was performed from 0.01 to 100 Hz and displayed in Fig. 4e and Fig. S5. Fig. 4e illustrates the Nyquist plots of representative PPy-0.5 and PPy-0.5/rGO NCF electrode. The equivalent circuit model is exhibited in the illustration of Fig. 4e, where R_s, R_{ct}, Z_w, C_{dl} and C typify the solution resistance, the intrinsic resistance of the material, charge

transfer resistance, the finite length Warburg ionic diffusion, and constant phase element of the double-layer capacitance and the faradic capacitance, respectively [45]. Both plots show a near semicircle in high-frequency range, the intercept of the semicircle at the real axis relates to the equivalent series resistance (R_s), the diameter of the semicircle typifies the charge transfer resistance (R_{ct}). From simulating, the values of R_s are 2.78 and 2.50 Ω for PPy-0.5 and PPy-0.5/rGO NCF electrodes, and the values of Rct are 0.58 and 0.43 Ω for the PPy-0.5 and PPy-0.5/rGO NCF electrode, respectively. Obviously, the R_s of the PPy-0.5/rGO nanocomposite is smaller than PPy-0.5 cotton fabric electrode, indicating the low solution resistance and intrinsic resistance of the electrode material. And the smaller R_{ct} of PPy-0.5/rGO NCF electrode suggests faster charge transfer. In the low-frequency, the PPy-0.5/rGO NCF shows a more vertical line than the PPy-0.5 fabric electrode, revealing the fast electron transport and ion diffusion. So the PPy-0.5/rGO NCF electrode is expected to be a potential candidate for supercapacitors electrode. Meanwhile, Fig. S5 shows the Nyquist plots of PPy-0.3, PPy-0.5, PPy-1.0, PPy-1.5 and PPy-2.0 cotton fabric electrodes. The values of R_s for PPy-0.3, PPy-0.5, PPy-1.0, PPy-1.5 and PPy-2.0 fabric electrodes are 2.80, 2.78, 2.84, 2.85 and 3.82 Ω, respectively, and the corresponding R_{ct} are 0.61, 0.58, 0.76, 0.81 and 1.29 Ω, respectively. The above results also demonstrate that the PPy-0.5 cotton fabric electrode has excellent electrochemical performance compared with other PPy cotton fabric electrodes, which matches well the results of CV and GCD.

The stability is also an important factor to affect the supercapacitors. Fig. 4f shows the curves of the PPy-0.5 and PPy-0.5/rGO NCF electrodes tested by cyclic voltammetry at 50 mV s^{-1} for 10000 cycles. Due to the self-activation of the electrodes, both the areal specific capacitances slightly increase in the first 300 (PPy-0.5) and 800 (PPy-0.5/rGO) cycles, respectively [36]. The capacitance retention of the PPy-0.5/rGO NCF electrode is 94.47% after 10000 cycles, which is much higher than PPy-0.5 cotton fabric electrode (87.92%). This is due to the reasons that, when pure PPy is used as electrode material for supercapacitors, volume swelling and shrinkage is easy to occur during charging and discharging, which results in inferior cycling stability and restricts its practical application [1]. When adding rGO, which is tightly integrated with PPy

(see Fig. 2c SEM) to prevent mechanical deformation of PPy due to swelling and shrinking. The cycling stability of the PPy-0.5/rGO NCF electrode is better than the reported long-life among similar electrodes and the obtained areal specific capacitance (9300 mF cm^{-2} at 1 mA cm^{-2}) in this work is much higher than the previously reported polypyrrole-based electrodes, which are exhibited in Table S1 for comparisons. The PPy-0.5/rGO NCF electrode has outstanding electrochemical performance due to the reasons (i): the homogeneous distribution of PPy nanoparticles on the rGO surface can make the active materials adequately meet with the electrolyte and shorten the charge transport pathways. (ii): the rGO forms a conductive network and acts as inner current collectors promoting electron transfer [39].

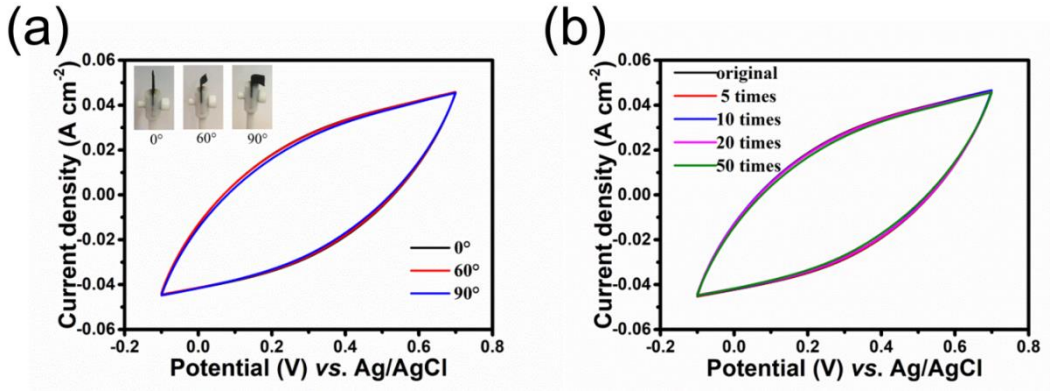

Fig. 5 (a) CV curves and photos of the PPy-0.5/rGO NCF electrode at various conditions. (b) CV curves of the PPy-0.5/rGO NCF electrode after water washing several times.

To satisfy the requirements of wearable supercapacitors, it is necessary for electrode materials to own superior flexibility as well as excellent electrochemical properties. The flexibility of the PPy-0.5/rGO NCF electrode can be evaluated by CV test under 0°, 60° and 90° states at 20 mV s^{-1}, as exhibited in Fig. 5a. The CV curves under different bending conditions keep almost unchanged, demonstrating that there are nearly no structure failure and small capacitance loss (After 90° bending, the capacitance retention rate is 95%), which is a very important requirement for the wearable applications. This further confirms that the PPy-0.5/rGO NCF electrode possesses good flexibility and can be integrated into various wearable and smart

electronic products. To verify the reuse capability of the nanocomposite, Fig. 5b presents the CV curves of the original and after washing times of PPy-0.5/rGO nanocomposite at 20 mV s^{-1}. After several times of washing, the curves have almost unchanged, demonstrating excellent reusability, which exploit a new pathway for the practical application of wearable devices.

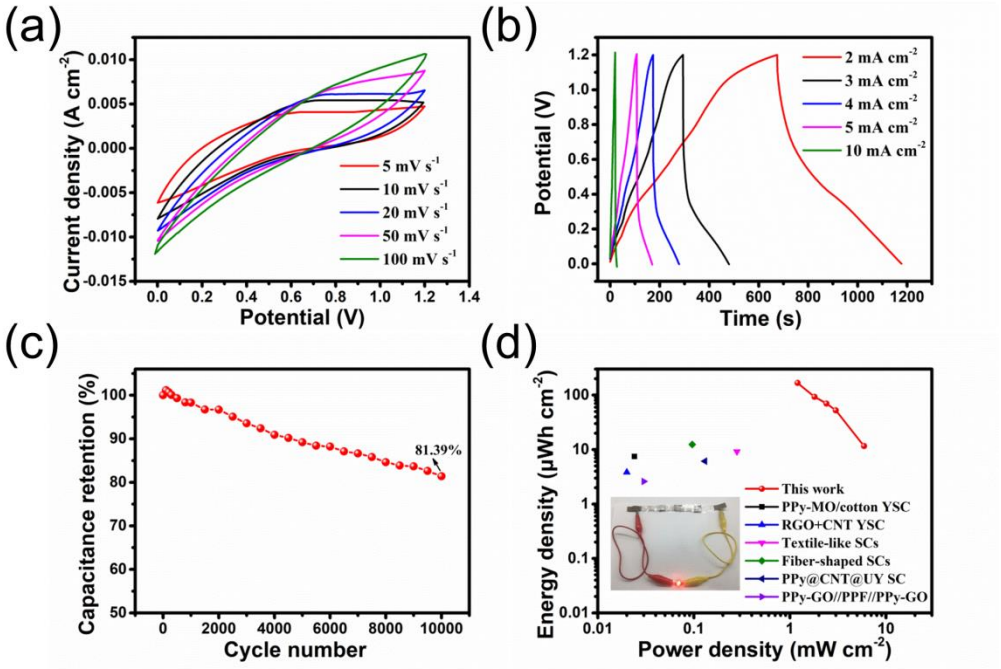

Fig. 6 (a) CV and (b) GCD curves of the symmetric all-solid-state supercapacitor (PPy/rGO-SC). (c) The cycle life of the PPy/rGO-SC was studied at 50 mV s^{-1}. (d) Ragone plot of the PPy/rGO-SC (inset: photograph of a LED lightened by three PPy/rGO-SC).

Further investigation of the practical application can be achieved from the electrochemical performance analysis based on a symmetric all-solid-state supercapacitor. The supercapacitor based on two PPy-0.5/rGO NCF electrodes, PVA/H_2SO_4 gel electrolyte, a separator and two conductive adhesives. The working area of PPy/rGO-SC is 1 cm^2 and the potential window is from 0 to 1.2 V. Fig. 6a displays the CV curves of the PPy/rGO-SC within the range of 5-100 mV s^{-1} and all the CV curves maintain nearly the same shapes, revealing excellent reversibly. In Fig. 6b, the nearly triangular and symmetric GCD curves of PPy/rGO-SC indicate excellent

rate capability. The corresponding areal capacitances are 836, 465, 350, 262 and 58 mF cm^{-2} at 2, 3, 4, 5 and 10 mA cm^{-2}, respectively.

Cyclic stability plays a crucial role in practicality. Fig. 6c exhibits the cycling property of PPy/rGO-SC evaluated by CV test after 10000 cycles with 50 mV s^{-1}. Thank to the self-activation, the capacitance increases in first 300 cycles, then gradually dropped to 81.39 % after 10000 cycles. Furthermore, Energy density (E) and power density (P) as two critical properties of PPy/rGO-SC can be calculated by formulas (3) and (4) and the corresponding Ragone plot of PPy/rGO-SC is displayed in Fig. 6d. The PPy/rGO-SC can obtain the maximal energy density of 167 μWh cm^{-2} with a power density of 1.20 mW cm^{-2}. Besides, the maximal power density can reach 6 mW cm^{-2} at an energy density of 11.66 μWh cm^{-2}. Compared with similar supercapacitors reported recently, such as PPy-MO/cotton-5 YSC (2.80 μWh cm^{-2} at 0.13 mW cm^{-2}) [46], RGO+CNT@CMC YCS (3.84 μWh cm^{-2} at 0.02 mW cm^{-2}) [47], Textile-like SCs (9.19 μWh cm^{-2} at 0.28 mW cm^{-2}) [48], fiber-shaped SCs (12.42 μWh cm^{-2} at 0.10 mW cm^{-2}) [49], PPy@CNT@UYSc (6.13 μWh cm^{-2} at 0.13 mW cm^{-2}) [50], PPy-GO//PPF//PPy-GO (2.60 μWh cm^{-2} at 0.03 mW cm^{-2}) [28], the PPy/rGO-SC in this work has the outstanding energy storage ability.

The good electrical performance of the PPy/rGO-SC is on account of the high load density and the large touch area between the gel electrolytes and fabric electrode. Moreover, after three devices are charged in series, an LED can be lighted, as displayed in the illustration of Fig. 6d. On the basis of our research results, the PPy-0.5/rGO NCF can be confirmed to be a hopeful candidate material for flexible devices.

4. Conclusion

In conclusion, this work presents a simple and low-cost preparation method to prepare the PPy/rGO NCF electrode by chemical polymerization. This PPy/rGO NCF electrode has not only high specific capacitance of 9300 mF cm^{-2} at 1 mA cm^{-2} and the excellent capacitance retention of 94.47% after 10000 cycles but also owns outstanding capacitance stability under different bending conditions and reuse capability. In addition, assembled symmetric all-solid-state supercapacitor achieves a high energy

density of 167 μWh cm^{-2} with the power density of 1.20 mW cm^{-2} and outstanding cycling stability.

Acknowledgments：

This work was supported by the NSFC (Nos. 11504229, 51602193), Shanghai "Chen Guang" project (16CG63). Open project of Key Laboratory of Artificial Structures and Quantum Control (Ministry of Education), Shanghai Jiao Tong University. Shanghai University of Engineering Science Innovation Fund for Graduate Students (17KY0512). The Talent Program of Shanghai University of Engineering Science, and the ESI Program of Shanghai University of Engineering Science (ESI201809, ESI201802). GH, PRS and DJLB acknowledge funding from the EPSRC (EP/R023581/1, EP/P009050/1).

REFERENCES:

[1] C. Sun, X. Li, Z. Cai, F. Ge, Carbonized cotton fabric in-situ electrodeposition polypyrrole as high-performance flexible electrode for wearable supercapacitor, Electrochimica Acta, 296 (2019) 617-626.

[2] N. Wang, X. Wang, Y. Zhang, W. Hou, Y. Chang, H. Song, Y. Zhao, G. Han, All-in-one flexible asymmetric supercapacitor based on composite of polypyrrole-graphene oxide and poly(3,4-ethylenedioxythiophene), Journal of Alloys and Compounds, 835 (2020) 155299.

[3] J. Yu, F. Xie, Z. Wu, T. Huang, J. Wu, D. Yan, C. Huang, L. Li, Flexible metallic fabric supercapacitor based on graphene/polyaniline composites, Electrochimica Acta, 259 (2018) 968-974.

[4] F. Qu, D. Jiang, Z. Liu, A. Zhang, Y. Zheng, Q. Jia, C. Li, J. Liu, Hierarchical polypyrrole/graphene/melamine composite foam for highly compressible all-solid-state supercapacitors, Electrochimica Acta, 353 (2020) 136600.

[5] Q. Lv, H. Hao, M. Ge, W. Li, S-doped graphene/mixed-valent manganese oxides composite electrode with superior performance for supercapacitors, Journal of Alloys

and Compounds, 819 (2020) 152970.

[6] K.S. Kumar, N. Choudhary, Y. Jung, J. Thomas, Recent Advances in Two-Dimensional Nanomaterials for Supercapacitor Electrode Applications, ACS Energy Letters, 3 (2018) 482-495.

[7] H. Hao, J. Wang, Q. Lv, Y. Jiao, J. Li, W. Li, I. Akpinar, W. Shen, G. He, Interfacial engineering of reduced graphene oxide for high-performance supercapacitor materials, Journal of Electroanalytical Chemistry, 878 (2020) 114679.

[8] C. Sun, X. Li, J. Zhao, Z. Cai, F. Ge, A freestanding polypyrrole hybrid electrode supported by conducting silk fabric coated with PEDOT:PSS and MWCNTs for high-performance supercapacitor, Electrochimica Acta, 317 (2019) 42-51.

[9] Y. Lin, H. Zhang, W. Deng, D. Zhang, N. Li, Q. Wu, C. He, In-situ growth of high-performance all-solid-state electrode for flexible supercapacitors based on carbon woven fabric/polyaniline/graphene composite, Journal of Power Sources, 384 (2018) 278-286.

[10] W. Wang, O. Sadak, J. Guan, S. Gunasekaran, Facile synthesis of graphene paper/polypyrrole nanocomposite as electrode for flexible solid-state supercapacitor, Journal of Energy Storage, 30 (2020) 101533.

[11] J. Lv, L. Zhang, Y. Zhong, X. Sui, B. Wang, Z. Chen, X. Feng, H. Xu, Z. Mao, High-performance polypyrrole coated knitted cotton fabric electrodes for wearable energy storage, Organic Electronics, 74 (2019) 59-68.

[12] Y. Shao, M.F. El-Kady, J. Sun, Y. Li, Q. Zhang, M. Zhu, H. Wang, B. Dunn, R.B. Kaner, Design and Mechanisms of Asymmetric Supercapacitors, Chemical Reviews, 118 (2018) 9233-9280.

[13] Q. Xue, J. Sun, Y. Huang, M. Zhu, Z. Pei, H. Li, Y. Wang, N. Li, H. Zhang, C. Zhi, Recent Progress on Flexible and Wearable Supercapacitors, Small, 13 (2017) 1701827.

[14] Y. Sun, D. Jia, A. Zhang, J. Tian, Y. Zheng, W. Zhao, L. Cui, J. Liu, Synthesis of polypyrrole coated melamine foam by in-situ interfacial polymerization method for highly compressible and flexible supercapacitor, Journal of Colloid and Interface Science, 557 (2019) 617-627.

[15] L. Yu, L. Hu, B. Anasori, Y.-T. Liu, Q. Zhu, P. Zhang, Y. Gogotsi, B. Xu, MXene-

Bonded Activated Carbon as a Flexible Electrode for High-Performance Supercapacitors, ACS Energy Letters, 3 (2018) 1597-1603.

[16] D. Islam, M.H. Uddin, B. Pan, M.M.A. Joy, Flexible and high-energy dense yarn-shaped supercapacitor based on Ni-carbon nanotubes framework, Chemical Physics Letters, 760 (2020) 138007.

[17] Z. Yang, Y. Jia, Y. Niu, Z. Yong, K. Wu, C. Zhang, M. Zhu, Y. Zhang, Q. Li, Wet-spun PVDF nanofiber separator for direct fabrication of coaxial fiber-shaped supercapacitors, Chemical Engineering Journal, 400 (2020) 125835.

[18] Q. Kang, J. Zhao, X. Li, G. Zhu, X. Feng, Y. Ma, W. Huang, J. Liu, A single wire as all-inclusive fully functional supercapacitor, Nano Energy, 32 (2017) 201-208.

[19] Y.-H. Lai, S. Gupta, C.-H. Hsiao, C.-Y. Lee, N.-H. Tai, Multilayered nickel oxide/carbon nanotube composite paper electrodes for asymmetric supercapacitors, Electrochimica Acta, 354 (2020) 136744.

[20] H. Shen, B. Wei, D. Zhang, Z. Qi, Z. Wang, Magnetron sputtered NbN thin film electrodes for supercapacitors, Materials Letters, 229 (2018) 17-20.

[21] Q. Xu, C. Wei, L. Fan, W. Rao, W. Xu, H. Liang, J. Xu, Polypyrrole/titania-coated cotton fabrics for flexible supercapacitor electrodes, Applied Surface Science, 460 (2018) 84-91.

[22] J. Lv, P. Zhou, L. Zhang, Y. Zhong, X. Sui, B. Wang, Z. Chen, H. Xu, Z. Mao, High-performance textile electrodes for wearable electronics obtained by an improved in situ polymerization method, Chemical Engineering Journal, 361 (2019) 897-907.

[23] A.J. Paleo, P. Staiti, A.M. Rocha, G. Squadrito, F. Lufrano, Lifetime assessment of solid-state hybrid supercapacitors based on cotton fabric electrodes, Journal of Power Sources, 434 (2019) 226735.

[24] H. Souri, D. Bhattacharyya, Highly Stretchable Multifunctional Wearable Devices Based on Conductive Cotton and Wool Fabrics, ACS Applied Materials & Interfaces, 10 (2018) 20845-20853.

[25] H. Jeon, J.M. Jeong, S.B. Hong, M. Yang, J. Park, D.H. Kim, S.Y. Hwang, B.G. Choi, Facile and fast microwave-assisted fabrication of activated and porous carbon cloth composites with graphene and MnO_2 for flexible asymmetric supercapacitors,

Electrochimica Acta, 280 (2018) 9-16.

[26] X. Liu, L. Xue, Y. Lu, Y. Xia, Q. Li, Fabrication of polypyrrole/multi-walled carbon nanotubes composites as high performance electrodes for supercapacitors, Journal of Electroanalytical Chemistry, 862 (2020) 114006.

[27] D. Zhu, X. Sun, J. Yu, Q. Liu, J. Liu, R. Chen, H. Zhang, D. Song, R. Li, J. Wang, Three-dimensional heterostructured polypyrrole/nickel molybdate anchored on carbon cloth for high-performance flexible supercapacitors, Journal of Colloid and Interface Science, 574 (2020) 355-363.

[28] N. Wang, G. Han, Y. Xiao, Y. Li, H. Song, Y. Zhang, Polypyrrole/graphene oxide deposited on two metalized surfaces of porous polypropylene films as all-in-one flexible supercapacitors, Electrochimica Acta, 270 (2018) 490-500.

[29] K. Kong, W. Xue, W. Zhu, W. Ye, Z. Zhang, R. Zhao, D. He, The fabrication of bowl-shaped polypyrrole/graphene nanostructural electrodes and its application in all-solid-state supercapacitor devices, Journal of Power Sources, 470 (2020) 228452.

[30] X. Guo, N. Bai, Y. Tian, L. Gai, Free-standing reduced graphene oxide/polypyrrole films with enhanced electrochemical performance for flexible supercapacitors, Journal of Power Sources, 408 (2018) 51-57.

[31] M. Xu, Y. Ma, R. Liu, Y. Liu, Y. Bai, X. Wang, Y. Huang, G. Yuan, Melamine sponge modified by graphene/polypyrrole as highly compressible supercapacitor electrodes, Synthetic Metals, 267 (2020) 116461.

[32] Y. Han, Z. Zhang, M. Yang, T. Li, Y. Wang, A. Cao, Z. Chen, Facile preparation of reduced graphene oxide/polypyrrole nanocomposites with urchin-like microstructure for wide-potential-window supercapacitors, Electrochimica Acta, 289 (2018) 238-247.

[33] M. Barakzehi, M. Montazer, F. Sharif, T. Norby, A. Chatzitakis, A textile-based wearable supercapacitor using reduced graphene oxide/polypyrrole composite, Electrochimica Acta, 305 (2019) 187-196.

[34] J. Chen, Y. Wang, J. Cao, Y. Liu, Y. Zhou, J.-H. Ouyang, D. Jia, Facile Co-Electrodeposition Method for High-Performance Supercapacitor Based on Reduced Graphene Oxide/Polypyrrole Composite Film, ACS Applied Materials & Interfaces, 9 (2017) 19831-19842.

[35] W.S. Hummers, R.E. Offeman, Preparation of Graphitic Oxide, Journal of the American Chemical Society, 80 (1958) 1339-1339.

[36] J. Li, H. Hao, J. Wang, W. Li, W. Shen, Hydrogels that couple nitrogen-enriched graphene with $Ni(OH)_2$ nanosheets for high-performance asymmetric supercapacitors, Journal of Alloys and Compounds, 782 (2019) 516-524.

[37] C. Yang, L. Zhang, N. Hu, Z. Yang, H. Wei, Y. Zhang, Reduced graphene oxide/polypyrrole nanotube papers for flexible all-solid-state supercapacitors with excellent rate capability and high energy density, Journal of Power Sources, 302 (2016) 39-45.

[38] S. Lyu, H. Chang, F. Fu, L. Hu, J. Huang, S. Wang, Cellulose-coupled graphene/polypyrrole composite electrodes containing conducting networks built by carbon fibers as wearable supercapacitors with excellent foldability and tailorability, Journal of Power Sources, 327 (2016) 438-446.

[39] J. Xu, D. Wang, Y. Yuan, W. Wei, L. Duan, L. Wang, H. Bao, W. Xu, Polypyrrole/reduced graphene oxide coated fabric electrodes for supercapacitor application, Organic Electronics, 24 (2015) 153-159.

[40] J. Zhu, T. Feng, X. Du, J. Wang, J. Hu, L. Wei, High performance asymmetric supercapacitor based on polypyrrole/graphene composite and its derived nitrogen-doped carbon nano-sheets, Journal of Power Sources, 346 (2017) 120-127.

[41] H. Zhou, G. Han, Y. Xiao, Y. Chang, H.-J. Zhai, Facile preparation of polypyrrole/graphene oxide nanocomposites with large areal capacitance using electrochemical codeposition for supercapacitors, Journal of Power Sources, 263 (2014) 259-267.

[42] M. Ge, H. Hao, Q. Lv, J. Wu, W. Li, Hierarchical nanocomposite that coupled nitrogen-doped graphene with aligned PANI cores arrays for high-performance supercapacitor, Electrochimica Acta, 330 (2020) 135236.

[43] H. Liu, J. Zhang, B. Zhang, L. Shi, S. Tan, L. Huang, Nitrogen-doped reduced graphene oxide-$Ni(OH)_2$-built 3D flower composite with easy hydrothermal process and excellent electrochemical performance, Electrochimica Acta, 138 (2014) 69-78.

[44] L. Ma, R. Liu, H. Niu, F. Wang, L. Liu, Y. Huang, Freestanding conductive film based

on polypyrrole/bacterial cellulose/graphene paper for flexible supercapacitor: large areal mass exhibits excellent areal capacitance, Electrochimica Acta, 222 (2016) 429-437.

[45] B. Liu, M. Yang, H. Chen, Y. Liu, D. Yang, H. Li, Graphene-like porous carbon nanosheets derived from salvia splendens for high-rate performance supercapacitors, Journal of Power Sources, 397 (2018) 1-10.

[46] C. Wei, Q. Xu, Z. Chen, W. Rao, L. Fan, Y. Yuan, Z. Bai, J. Xu, An all-solid-state yarn supercapacitor using cotton yarn electrodes coated with polypyrrole nanotubes, Carbohydrate Polymers, 169 (2017) 50-57.

[47] L. Kou, T. Huang, B. Zheng, Y. Han, X. Zhao, K. Gopalsamy, H. Sun, C. Gao, Coaxial wet-spun yarn supercapacitors for high-energy density and safe wearable electronics, Nature Communications, 5 (2014) 4754.

[48] K. Liu, Y. Yao, T. Lv, H. Li, N. Li, Z. Chen, G. Qian, T. Chen, Textile-like electrodes of seamless graphene/nanotubes for wearable and stretchable supercapacitors, Journal of Power Sources, 446 (2020) 227355.

[49] H. Wei, H. Hu, J. Feng, M. Zhang, T. Hua, Yarn-form electrodes with high capacitance and cycling stability based on hierarchical nanostructured nickel-cobalt mixed oxides for weavable fiber-shaped supercapacitors, Journal of Power Sources, 400 (2018) 157-166.

[50] J. Sun, Y. Huang, C. Fu, Z. Wang, Y. Huang, M. Zhu, C. Zhi, H. Hu, High-performance stretchable yarn supercapacitor based on PPy@CNTs@urethane elastic fiber core spun yarn, Nano Energy, 27 (2016) 230-237.